

# Lawrence Berkeley National Laboratory

## LBL Publications

### Title

Compact Spreader Schemes

### Permalink

<https://escholarship.org/uc/item/2ss5p9hk>

### Journal

Nuclear Instruments and Methods in Physics Research Section A: Accelerators, Spectrometers, Detectors and Associated Equipment, 768(Dec. 21 2014)

### Authors

Placidi, M.  
Jung, J.-Y.  
Ratti, A.  
et al.

### Publication Date

2014-12-21

This document was prepared as an account of work sponsored by the United States Government. While this document is believed to contain correct information, neither the United States Government nor any agency thereof, nor The Regents of the University of California, nor any of their employees, makes any warranty, express or implied, or assumes any legal responsibility for the accuracy, completeness, or usefulness of any information, apparatus, product, or process disclosed, or represents that its use would not infringe privately owned rights. Reference herein to any specific commercial product, process, or service by its trade name, trademark, manufacturer, or otherwise, does not necessarily constitute or imply its endorsement, recommendation, or favoring by the United States Government or any agency thereof, or The Regents of the University of California. The views and opinions of authors expressed herein do not necessarily state or reflect those of the United States Government or any agency thereof or The Regents of the University of California.

# COMPACT SPREADER SCHEMES

M. Placidi, J-Y. Jung, A. Ratti and C. Sun

Lawrence Berkeley National Laboratory, Berkeley, CA 94720, U.S.A.

This paper describes beam distribution schemes adopting a novel implementation based on low amplitude vertical deflections combined with horizontal ones generated by Lambertson-type septum magnets. This scheme offers substantial compactness in the longitudinal layouts of the beam lines and increased flexibility for beam delivery of multiple beam lines on a shot-to-shot basis. Fast kickers (FK) or transverse electric field RF Deflectors (RFD) provide the low amplitude deflections. Initially proposed at the Stanford Linear Accelerator Center (SLAC) as tools for beam diagnostics and more recently adopted for multiline beam pattern schemes, RFDs offer repetition capabilities and a likely better amplitude reproducibility when compared to FKs, which, in turn, offer more modest financial involvements both in construction and operation. Both solutions represent an ideal approach for the design of compact beam distribution systems resulting in space and cost savings while preserving flexibility and beam quality.

## INTRODUCTION

Modern Linac-based Free Electron Laser (FEL) systems are often equipped with multiple beam lines which require a beam switchyard (BSY) to distribute electron bunches from the Linac to individual FELs. The BSY design is challenging, as it requires not only to preserve beam quality and provide flexible bunch repetition rate, but also to meet the physical constraint of the facility site. In this paper we present designs of compact Beam Switchyard (BSY) systems. Fast Switching Devices (FSD) like Fast Kickers (FK) or RF Deflectors (RFD) initiate a low-amplitude vertical splitting. Septum magnets installed downstream as the vertical separation between the trajectories matches the magnet apertures provide the first horizontal deflections. The resulting schemes represent an ideal solution for the design of compact beam distribution systems resulting in space and cost savings while preserving flexibility and beam quality in a variety of Beam Switch Yard topologies.

Transverse deflecting RF structures, originally proposed at SLAC [1] and at the Thomas Jefferson National Accelerator Facility (TJNAF) [2] as tools for beam separation, space phase diagnostics and bunch length measurements [3,4], have subsequently found additional applications as fast switching devices in beam distribution systems for multiple beam lines layouts [5,6]. The adoption of transverse RF deflectors allows distributing electron bunches with on-demand repetition rates in each line, well above the few hundred kHz limit likely represented by fast kickers. In addition, the steady state nature of the CW transverse fields provides higher deflection stability and shot-to-shot reproducibility as compared to those achievable with fast kickers where the deflecting pulses are created at every bunch passage. Beam distribution schemes adopting cascading RF deflectors have been discussed in [7] and complement this paper.

Conversely, the technology associated with stripline- and ferrite-based Fast Kickers is well developed and their use represents a more attractive solution from the financial investment point of view.

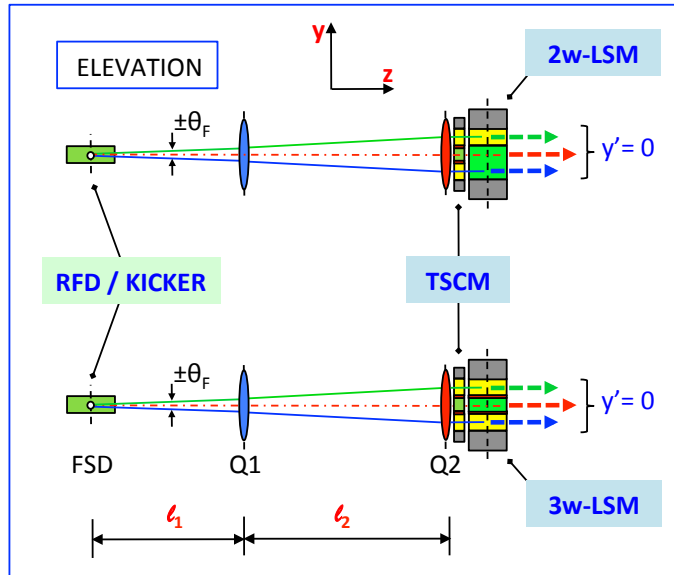
Issues related to Machine Protection also play an important role in the choice between the two options.

## THE INITIAL SPLITTING MODULE

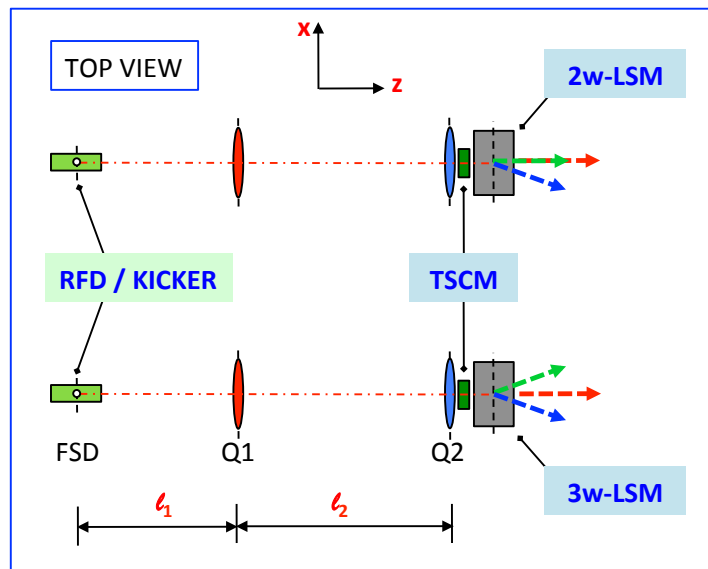
Stability and reproducibility criteria require the deflections from the fast switching devices to be of the order of 1-mrad or less. A BSY layout based on reduced amplitude initial horizontal deflections would involve very long beam lines to provide clearance to the downstream deflecting and focusing elements.

Schemes involving an initial splitting in the vertical direction further combined with horizontal deflections provided by properly designed Lambertson-type septum magnets (LSM) located at a short distance downstream offer instead options for substantial reductions in the longitudinal extent of the beam lines. The LSM thin septum offers instead options for substantial reductions in the longitudinal extent of the beam lines. The LSM thin septum accepts a contained vertical separation between the trajectories allowing the magnet to be installed at a relatively short distance from the fast switching devices, resulting in a more compact longitudinal footprint of the BSY layout.

51 In the basic splitting module scheme shown in Figures 1 and 2 an initial section produces three vertical  
 52 trajectories selectively deflected by the LSMs. Two-way and three-way Lambertson magnet options can be  
 53 adopted depending on the chosen BSY topology.



71 **Fig. 1:** Elevation of the basic module of the initial vertical splitting scheme. A Fast Switching Device (FSD)  
 72 vertically splits an incoming bunch train into three trajectories with a small amplitude angle  $\pm\theta_F$ . The initial  
 73 slopes, enhanced by the vertically defocusing quadrupole Q1, are compensated at the entrance of the LSM  
 74 downstream.



91 **Fig. 2:** Top view of the basic module of the initial vertical splitting scheme showing the role of two- or a three-  
 92 way LSM installed at a relatively short distance from the FSD.

94 *Vertical splitting*

95 A Fast Switching Device, either a bipolar kicker or an RFD, vertically splits an incoming bunch train into three  
 96 trajectories, two deflected and one straight. The small amplitude deflections are enhanced by the vertically

97 defocusing quadrupole  $Q_1$  while the  $Q_2$  location defines the trajectories separation  $\Delta y$ . A Twin Septum Corrector  
 98 Magnet (TSCM) or  $Q_2$  compensate\* the slopes  $\Delta y'$  at the LSM entrance.  
 99 The scheme consists of a telescopic arrangement of elements governed by the vertical transfer matrix from the  
 100 FSD to the LSM with the constraints:

$$102 \quad R_{12}^y = \Delta y / \theta_F, \quad R_{22}^y = 0. \quad (1)$$

103 Solving (1) with the compact arrangement condition

$$105 \quad l_1 + l_2 = \min \quad (2)$$

106 gives, in thin lens approximation:

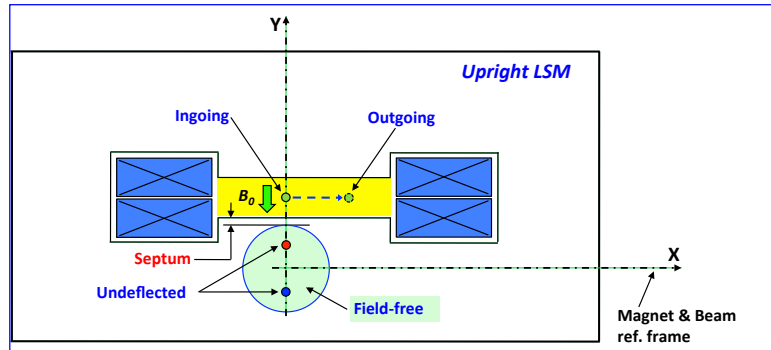
$$108 \quad l_{1,2} \equiv l = -f_1 + \sqrt{f_1(f_1 + R_{12}^y)} \quad , \quad f_2 = l \left( \frac{2f_1 + l}{f_1 + l} \right) \quad (3)$$

109 where  $f_1$  and  $f_2$  are the  $Q_1$  and  $Q_2$  focal lengths.

110 A numerical example for  $R_{12}^y = 15.0$ -mm/mrad and a conservative  $f_1 = 1.48$ -m gives  $l = 3.46$ -m and  $f_2 = 4.34$ -m. The  
 111 quoted focal lengths are consistent with a 0.6-T  $B_{TIP}$  value at 4-GeV beam energy for 0.15-m long standard  
 112 quadrupoles with 20-mm and 60-mm respective bore diameters offering comfortable apertures for the local  
 113 trajectory separation.

### 115 *Horizontal Deflection: Dedicated Magnets*

116 LSM magnets provide the first horizontal deflections. A typical two-way LSM is shown in Figure 3 in upright  
 117 configuration. In this design, originally conceived for the three-way RFD deflecting scheme of the Next  
 118 Generation Light Source (NGLS) project at the Lawrence Berkeley National Lab, the zero-field passage has a  
 119 relatively large internal diameter to accommodate two un-deflected trajectories while the other one is right  
 120 deflected to create the first branch of the spreader. A 2-mm thin septum separates the deflecting gap from the  
 121 field-free region.



132 **Fig. 3:** Cross section of a two-way upright LSM magnet. The top trajectory (green) is deflected to the right while  
 133 the two others travel un-deflected in the field-free channel.

136 A Poisson's simulation for the LSM of Figure 3 anticipates (Figure 4) a residual field in the field-free region with  
 137 components

$$138 \quad B_x^{res} = 0.74G, \quad B_y^{res} = 2.4G. \quad (4)$$

140 The 0.33-T design figure of the main deflecting field and the  $<2.5$ -G residual B-field in the field-free region  
 141 provide 25-mrad and about 20- $\mu$ rad deflections respectively for a 4-GeV beam. A parameter list for the two-way  
 142 LSM is given in Table 1.

\* Arguments supporting slope compensations are developed in a subsection below.

143  
 144  
 145  
 146  
 147  
 148  
 149  
 150  
 151  
 152  
 153  
 154  
 155  
 156  
 157  
 158  
 159  
 160  
 161  
 162  
 163  
 164  
 165  
 166  
 167  
 168  
 169  
 170  
 171  
 172  
 173  
 174  
 175  
 176  
 177  
 178  
 179  
 180

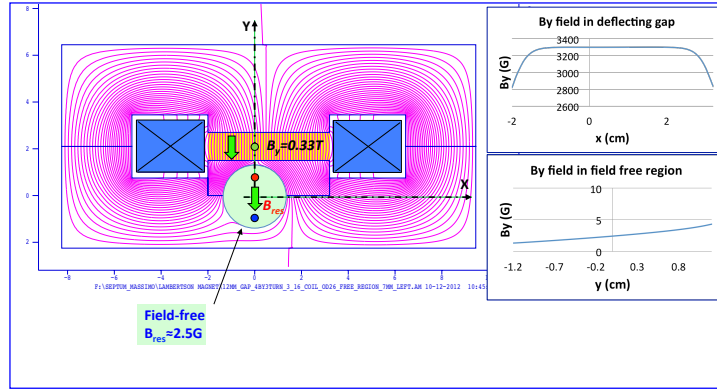


**Fig. 4:** Poisson simulation of the field strengths for the magnetic circuit of Figure 3. A 2-mm thin septum contains the residual B-field down to  $0.8 \times 10^{-3}$  the main one.

**Table 1:** Parameter list for a two-way LSM.

Two-way Lambertson Parameters		
Magnet type	Window frame	
Deflection	mrad	25.0
Energy	GeV	4.0
Incoming beam sep.	mm	$\pm 15.0$
Field strength	Tm	0.330
Eff. Length	m	1.0
Septum	mm	2.0
Defl. Gap height	mm	12.0
Main B-field	T	0.33
Residual B-field	G	$\sim 3$
Coils		2 x 10 turns
Magnet Current	A	158.0
Magnet Power	kW	1.27

In compact beam distribution schemes it is sometimes useful to concentrate two horizontal opposite deflections in a single LSM still leaving the option for an un-deflected trajectory. A design of a three-way LSM, with a central zero-field region separating two deflecting gaps, is shown in Figure 5. The cylindrical vacuum pipe is installed in a rectangular cross section passage for easier yoke construction.

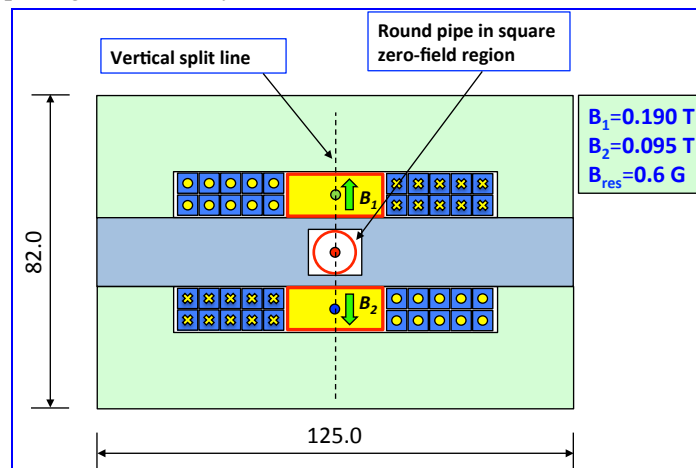
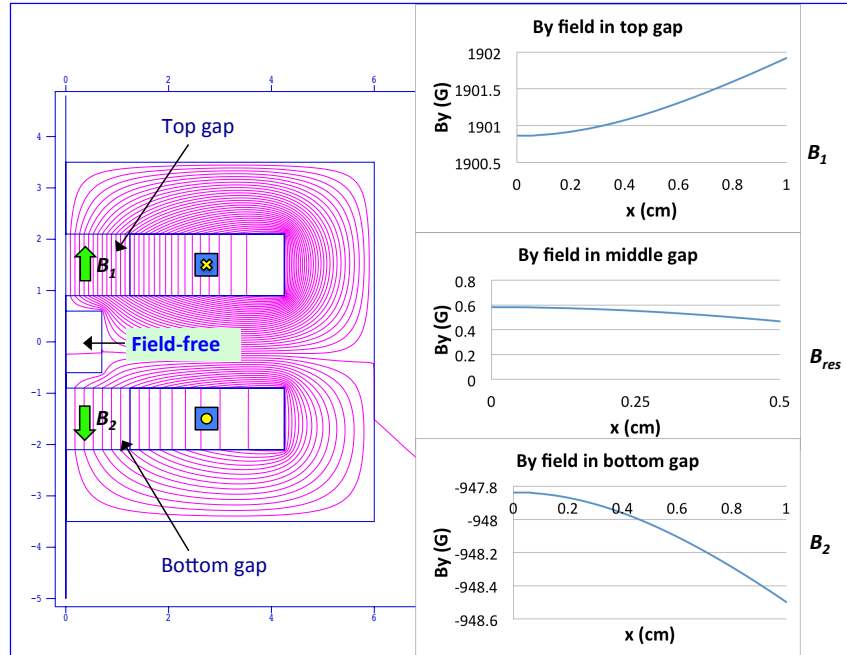


**Fig. 5:** Cross section of a three-way “asymmetric” LSM. The magnet can provide opposite deflection differing by up a factor of two while keeping the residual field below 0.6-G. Dimensions are in mm.

181 In a basic scheme the same amplitude opposite B-fields fully compensate the residual field in the central passage.  
 182 A more flexible solution is proposed with the present “asymmetric deflection” design where different amplitude  
 183 deflections are available. The 0.7-m long magnet provides up to 5- and 10-mrad opposite deflections to a 4-GeV  
 184 beam. The Poisson-simulated magnet properties (Figure 6) anticipate a  $\sim 0.6$ -G residual field in the central passage  
 185 and a  $0.7 \times 10^{-3}$  radial non-homogeneity of the main deflecting fields. Table 2 gives a parameter list for the three-  
 186 way LSM sketched in Figure 5.



203 **Fig. 6:** Poisson simulation for the three-way LSM cut at the vertical symmetry plane. The B-field distributions in  
 204 the two deflecting gaps are plotted together with the associated residual field in the zero-field channel.

205  
 206  
 207 **Table 2:** Parameter list for a three-way LSM.

Three-way Lambertson Parameters		
Magnet type	Twin window frame	
Deflection	mrad	10.0 / 5.0
Energy	GeV	4.0
Incoming beam sep.	mm	$\pm 15.0$
Field strength	Tm	0.133 / 0.067
Eff. Length	m	0.70
Septum	mm	3.0
Defl. Gap height	mm	12.0
Main B-field	T	0.19 / 0.095
Residual B-field	G	$\sim 0.6$
Coils		2 x 10 turns
Current	A	184.0 / 92.0
Power	kW	0.595 / 0.149

222 The Twin Septum Magnet (TSM) shown in Figure 7 is a simplified version of the three-way LSM that can be  
 223 used to provide simultaneous opposite deflections to two incoming trajectories. The two deflecting gaps are  
 224 separated by a thicker septum than in the LSM and provide opposite sign B-fields. A Poisson simulated TSM  
 225 performance suggests an 8-mm septum thickness in the  $2 \times 0.19$ -T equal B-fields configuration, and 6-mm in the  
 226 non-equal deflection case of Figure 5, to contain the field in the septum around 1.3-T. With the shown geometry  
 227 the incoming beam separation is in the range of 18- to 20-mm. A parameter list for the TSM is given in Table 3.

228

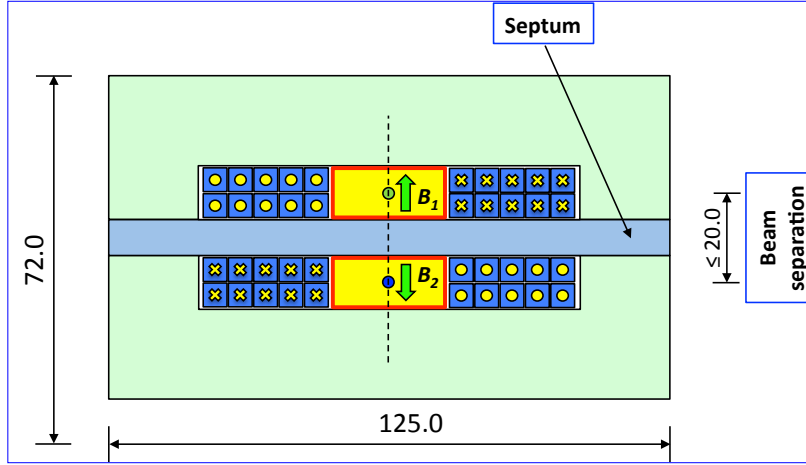


**Fig. 7:** Cross section of a Twin Septum Magnet (TSM) providing equal amplitude opposite deflection. Optional non-equal deflections are possible requiring smaller septum thickness. Dimensions in mm.

**Table 3:** Parameter list for a two-way TSM.

TSM Parameters		
Magnet type	Twin window frame	
Deflection	mrad	±10.0
Energy	GeV	4.0
Incoming beam sep.	mm	±10.0
Field strength	Tm	0.133
Eff. Length	m	0.70
Septum	mm	8.0
Defl. Gap height	mm	12.0
Main B-field	T	0.19
Coils	2 x 10 turns	
Current	A	184.0
Power	kW	1.2

A Poisson simulation for the TSM anticipates a B-field constant across the gaps width with coefficients

$$G_y = 1.1 \cdot 10^{-2} \text{ G/mm}, \quad S_y = 1.0 \cdot 10^{-2} \text{ G/mm}^2. \quad (5)$$

### SLOPE COMPENSATION

In a vertical initial splitting scheme it is essential to foresee early compensation of the vertical slopes of the trajectories deflected by the FSDs to avoid the development of large offsets along the beam path and the use of wide aperture correctors downstream. Slope compensations can be achieved in different ways.

#### *Rolled LSMs*

An LSM rotated around the beam direction (Figure 8) introduces a vertical steering via the horizontal component of the main B-field.

The amount of rotation depends on the required steering amplitude and is usually in the range of a few degrees. The roll direction defines the sign of the compensation steering. From the cyclotron equation

$$p = \beta E/c = eB\rho \quad (6)$$

the development of the trajectory deflections along the integrated field strengths at a given beam energy  $E$  reads, in practical units (relativistic case,  $\beta=1$ ):



280

$$\theta_{x,y}(s) = \frac{c \int B_{y,x} ds}{\beta E l e} \approx 0.3 L_m \frac{B_{y,x}}{E} \quad [\text{GeV}, \text{T}, \text{m}] \quad (7)$$

281

282

283

where  $\theta_{x,y}$  are the LSM deflections associated to the  $B_{y,x}$  components of the main field assumed constant along the magnet effective length  $L_m$ . The roll angle  $\alpha$  is then

284

$$\alpha = \tan^{-1} \left( \frac{B_x}{B_y} \right) = \tan^{-1} \left( \frac{\theta_y}{\theta_x} \right). \quad (8)$$

285

286

287

288

289

290

291

292

293

294

295

296

297

298

299

300

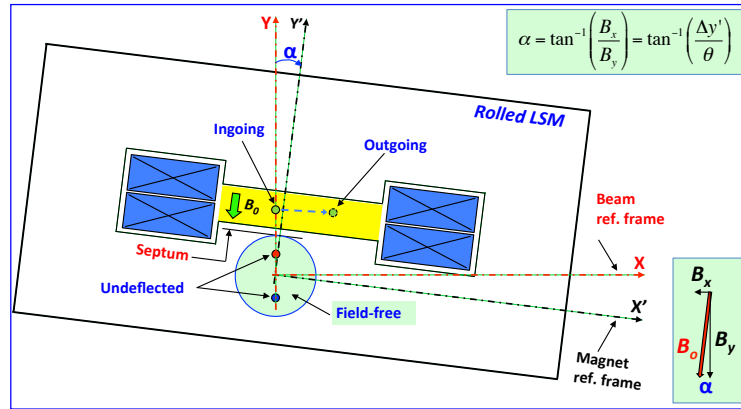


**Fig. 8:** Vertical steering from a rotated LSM.

301

302

303

To provide the same deflection as an upright LSM, the rolled LSM must have the same vertical B-field component and its excitation is returned according to

304

$$B_0^{roll} = \frac{B_0^{upr}}{\cos \alpha}. \quad (9)$$

305

### Septum Corrector Magnets

306

307

308

309

310

311

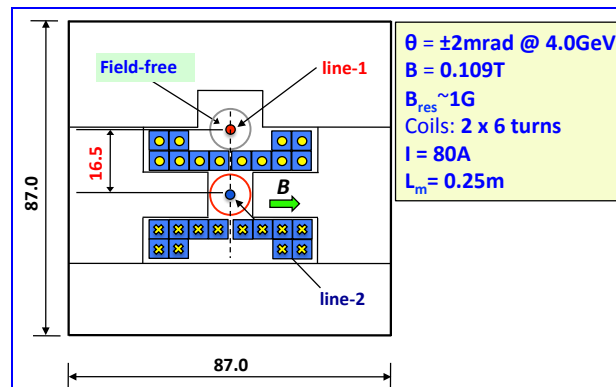
312

313

Septum-type Corrector Magnets (SCM) can be used to selectively compensate the slopes of trajectories spatially very close to each other, when their separation prevents the use of standard, single beam correctors. In this case the steering direction lies in the same plane of the incoming trajectories so the septum thickness and the beams separation are set by the size of the coil conductor, differently from the LSM case. The following examples deal with trajectory separation and steering direction in the vertical plane.

The septum corrector sketched in Figure 9 vertically steers the incoming line-2 parallel to the un-deflected line-1.

The 5-mm septum thickness imposes a ~16 mm separation between the incoming trajectories.



314

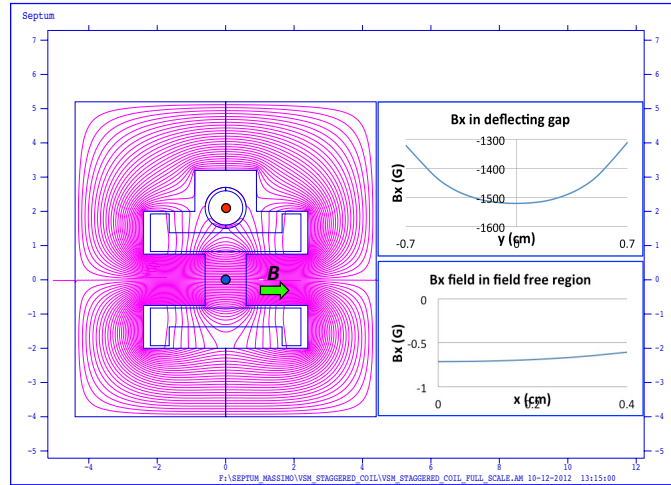
315

**Fig. 9:** Cross section of a compact SCM corrector for the vertical steering of line 2. Dimensions are in mm.

316 The Poisson simulation of Figure 10 anticipates a  $\sim 1$ -G residual field in the central region and a 0.1-T main B-  
 317 field in the deflecting gaps with a 6-polar coefficient

318 
$$S_y \cong 2.8 \text{ G/mm}^2 . \quad (5')$$

319  
320  
321  
322  
323  
324  
325  
326  
327  
328  
329  
330  
331  
332

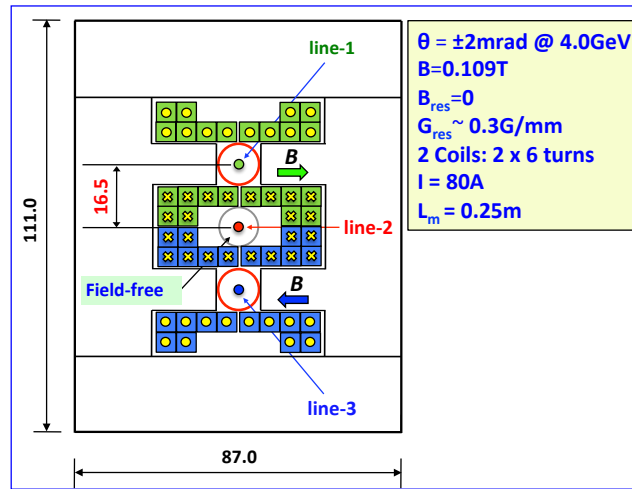


333 **Fig. 10:** Poisson simulation for the SCM vertical corrector. Shown is one quarter of the symmetric structure.

334  
335  
336

337 A twin septum corrector (TSCM) can be used to compensate the vertical slopes of the two trajectories at the exit  
 338 of the vertically focusing  $Q_2$  in the scheme of Figure 1, if the latter is part of a FODO system. A sketch of a  
 339 TSCM magnet in “divergent” configuration is shown in Figure 11. Opposite sign B-fields provide independent  
 340 converging or diverging vertical deflections to line-1 and line-3 and fully compensate the residual field in the  
 341 central gap.

342  
343  
344  
345  
346  
347  
348  
349  
350  
351  
352  
353  
354  
355  
356



357 **Fig. 11:** Cross section of a compact TSCM corrector. Opposite sign B-fields provide converging or diverging  
 358 vertical deflections and compensate the residual field in the central gap. Dimensions are in mm.

359  
360  
361  
362

360 The Poisson simulation in Figure 12 anticipates the behavior of the main and residual horizontal B-fields  
 361 characterized by the coefficients

363 
$$G_y^{main} = 213.2 \text{ G/mm} , S_y^{main} = -6.1 \text{ G/mm}^2$$
  
 364 
$$G_y^{res} = 0.28 \text{ G/mm} . \quad (5'')$$

365

366  
 367  
 368  
 369  
 370  
 371  
 372  
 373  
 374  
 375  
 376  
 377  
 378  
 379  
 380  
 381  
 382  
 383  
 384  
 385  
 386  
 387  
 388  
 389  
 390  
 391  
 392  
 393  
 394  
 395  
 396  
 397  
 398  
 399  
 400  
 401  
 402  
 403  
 404  
 405  
 406  
 407  
 408  
 409  
 410  
 411  
 412  
 413  
 414

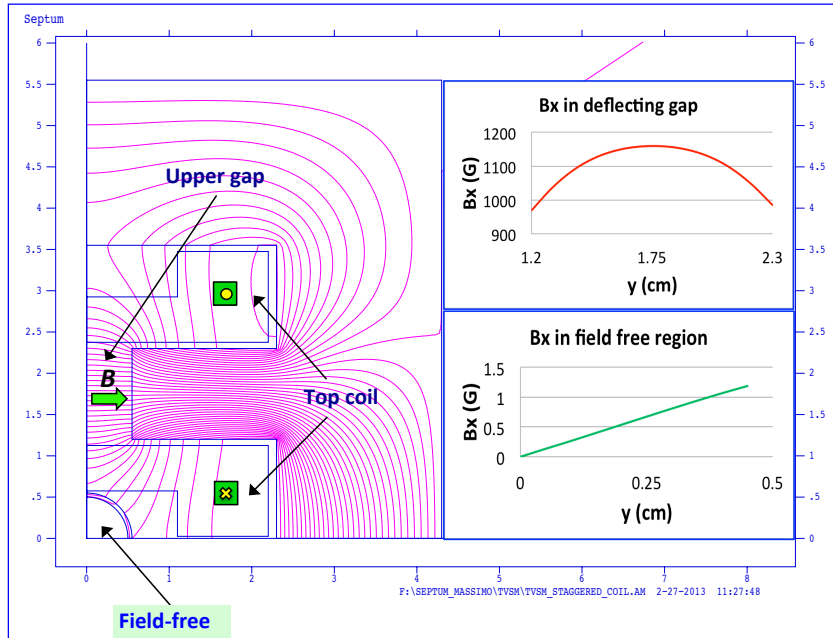


**Fig. 12:** Poisson simulation for one quarter of the symmetric structure of the TSCM corrector.

### BSY TOPOLOGIES

Several BSY topologies can be realized combining the initial vertical splitting from Fast Deflecting Switches with dedicated deflecting elements like the “two- or “three-way” LSMs and the TSM. Examples of possible BSY layouts are sketched in Figure 13. Figure 13a) shows a possible evolution of the original right-side oriented scheme of the NGLS Spreader involving two and three-way LSMs. In Figure 13b) “three-way” LSMs and TSMs combine into a layout symmetric to the central line.

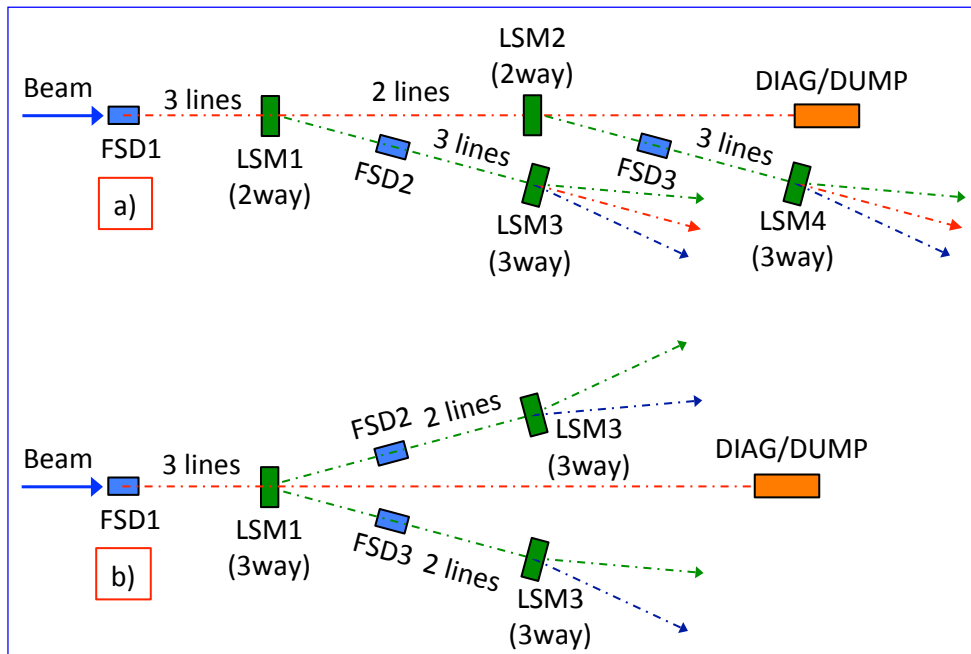


**Fig. 13:** Examples of BSY layouts involving initial vertical splitting from Fast Switching Devices (FSD) followed by horizontal deflections from combinations of Two- and Three-way Lambertson Septum Magnets (LSM).

415  
416  
417  
418  
419  
420  
421  
422  
423  
424  
425

## SUMMARY

Compact beam spreader schemes combining vertical, small amplitude initial deflections from fast kickers or RF deflectors with horizontally bending Lambertson-type septum magnets offer several advantages in the design of compact beam distribution systems requiring flexibility and beam quality. The intrinsic nature of the CW RFD option is expected to offer higher deflection stability and reproducibility as compared to those from fast kicker technology and does not suffer from limitations in bunch repetition rates. Fast kicker solutions offer a much lower financial investment, both in construction and operation, when dealing with repetition rates in a few hundred kHz range. In both cases BSY layouts adopting vertical initial splitting schemes can feed multiple beam lines in very compact beam distribution schemes.

426

## ACKNOWLEDGMENTS

427 The authors wish to thank P. J. Emma and J. M. Byrd for sharing many useful discussions, as well as D. S. Robin  
428 for support with beam dynamic issues and transport studies for the NGLS Project. The NGLS management  
429 encouraged and funded this study. This work was supported by the Director, Office of Science, Office of High  
430 Energy Physics, of the U.S. Department of Energy under Contract No. DE-AC02-05CH11231.

431

432

## REFERENCES

433

[1] G. A. Loew, O. H. Altenmueller, "*Design and Applications of R.F. Deflecting Structures at SLAC*",  
434 PUB-135, Aug. 1965.

435

[2] C. Leemann, C. G. Yao, "*A Highly Effective Deflecting Structure*", CEBAF TN-90-217, April 25,  
436 1990.

437

[3] R. Akre *et al.*, "*A Transverse Deflecting Structure for Bunch Length and Phase Space Diagnostics*",  
438 SLAC-PUB-8864, June 2001.

439

[4] S. Belomestnykh *et al.*, "*Deflecting Cavity for Beam Diagnostics in ERL Injector*", PAC07,  
440 Albuquerque, NM, USA.

441

[5] C. Hovater *et al.*, "*The CEBAF RF Separator System*", JLAB-ACC-96-18.

442

[6] R. Kazimi, "*Simultaneous Four-Hall Operation for 12 GeV CEBAF*", IPAC13, Shanghai, China.  
443 THPFI091.

444

[7] L. Doolittle *et al.*, "*Cascading RF Deflectors in Beam Spreader Schemes*", to be published.